

Theoretical analysis of humidification – dehumidification process in an open type solar desalination system

Salman H. Hammadi

Department of Mechanical Engineering, Engineering College, Basrah University, Iraq

ARTICLE INFO

Keywords:

Active solar still
Open-type solar still
Solar humidification-dehumidification

ABSTRACT

A theoretical study of humidification – dehumidification (HDH) process in transient mode inside an open solar distiller is presented. Energy and mass balances of the water layer, airstream, and glass cover of the distiller are formulated and numerically simulated. Dry air enters into the distiller is heated up and humidified by solar radiation. When the glass temperature is lower than or equal to the dew point of the humid air, the vapor condenses on the inner side of the glass cover and runs down where the fresh water is collected. The results show that the productivity of fresh water is strongly affected by the water, air, and glass temperatures and the maximum productivity achieved in March was 2.2 kg/m² day. The increase in air velocity inside the solar distiller increases the evaporation rates and decreases the productivity. The distiller length required to reach the saturated state essentially depends on the air velocity and the water temperature. A comparison of the current analysis with other works showed a good agreement.

Nomenclature

A	area (m ²)
C _{pf}	specific heat of air (J/kg °C)
C _w	specific heat of water (J/kg °C)
h _a	heat transfer coefficient between glass and surrounding (W/m ² °C)
h _w	heat transfer coefficient between water and air (W/m ² °C)
h _f	heat transfer coefficient between air and glass (W/m ² °C)
h _{fg}	latent heat of evaporation (J/kg)
h _g	enthalpy of saturated vapor (J/kg)
h _v	enthalpy of vapor (J/kg)
I	total solar radiation (W/m ²)
I _{df}	diffused solar radiation (W/m ²)
I _{dr}	direct solar radiation (W/m ²)
I _{sc}	solar constant (W/m ²)
L	distiller length (m)
m _a	air mass (-)
\dot{m}_f	air mass flowrate (kg/s)
m _{co}	condensation rate(kg/s)
m _{ev}	evaporation rate(kg/s)
P	atmospheric pressure (N/m ²)
P _{fis}	saturated pressure at inlet air temperature (N/m ²)
P _{fo}	vapor pressure at outlet air temperate(N/m ²)
P _{fos}	saturated pressure at outlet air temperature (N/m ²)
P _g	saturated pressure at the glass temperature(N/m ²)
P _{ws}	saturated pressure at the water temperature (N/m ²)

Q_{cg}	convection heat transfer between air and glass (W)
Q_{cw}	convection heat transfer between water and air (W)
Q_{eg}	condensation heat transfer between
$T_{a,max}$	monthly maximum ambient temperature ($^{\circ}C$)
$T_{a,min}$	monthly minimum ambient temperature ($^{\circ}C$)
T_a	ambient temperature ($^{\circ}C$)
T_{dp}	dew point temperature ($^{\circ}C$)
T_f	airstream temperature ($^{\circ}C$)
\bar{T}_f	average air temperature ($^{\circ}C$)
T_g	glass temperature ($^{\circ}C$)
T_w	water temperature ($^{\circ}C$)t time (s)
U_a	wind velocity (m/s)
U_f	airstream velocity (m/s)
w	humidity ratio (kg/kg of dry air)
\bar{w}_f	average humidity ratio of air (kg/kg of dry air)
x	horizontal coordinate (m)
y	day length (hr.)

Greek letters

α_g	glass absorptivity (-)
α_w	water absorptivity (-)
β	altitude angle (degree)
ϕ	relative humidity (-)
δ	declination angle (degree)
ℓ	latitude angle (degree)
λ	hour angle (degree)
τ_g	glass transmissivity (-)

Subscript

f	air inside the distiller
g	glass
i	inlet
o	outlet
s	saturation
w	water air and glass (W)
Q_{ew}	evaporative heat transfer between water and air (W)

1. Introduction

The fresh water demand is continuously increasing around the world because of the population explosion and Industrial development. The conventional systems for water desalination are mechanically complicated and energy intensive with a high level of pollutants. Solar energy can be employed to make the desalination process cheaper and more environmentally friendly in sunny and remote regions. Solar assisted humidification and dehumidification technique (SHD) is widely employed to the desalination process. In such technique, the ambient air is humidified by warm water heated up by the solar radiation. The humid air dehumidified when it touches a surface at a temperature lower than the dew point of the humid air and the vapor precipitates as freshwater on the surface.

The main part of the previous studies relating to the solar humidification-dehumidification systems deals with the passive type and neglecting the effect of air motion inside the system. The present study is an addition to some studies available in the literature dealing with the effect of forced convection within the open-type solar desalination system. Among these studies, the work by Ali [1] that experimentally studied the effect of air motion inside a 3 m² solar still on the still performance. His results show that the distilled water output in the case with fan and insulated air channel is nearly 29.7% higher than the output from the conventional design. Ali [2] presented a mathematical model to predict the performance of the solar still using forced convection inside the solar still to enhance the productivity of the still. He showed that about 220% enhancement in the productivity with increasing Reynolds number to 52,800.

Ali [3] studied the effect of forced convection inside a solar still on heat and mass transfer coefficient. Different parameters were studied, such as fluting of the water surface due to the air motion, air turbulent eddies, vapor velocity inside the still and accumulation of non-condensable gas. He concluded that the increase in the productivity of the solar still is mainly due to the enhancement in the heat and mass transfer coefficients due to the existence of the air-vapor mixture turbulent motion inside the still. Sartori [4] presented a theoretical comparison between the thermal behavior of a basin type solar still and that from a solar evaporator. Both the still and the evaporator are made of glass fiber and thermally insulated with 0.045 m of glass wool at bottom and sides. Each water

surface has one square meter and its layer 0.04 m. A common 3 mm thick window glass is employed for the still cover. He found that the evaporation in solar stills is much less than that in open evaporation despite the higher water temperatures in the former system. For relatively high water temperatures of each system, the evaporative fraction is equivalent to more than 50% of the corresponding total heat transfer rate.

Radhwan [5] presented a transient analysis of a stepped solar still for heating and humidifying agriculture greenhouses. Air circulated inside the still where it is heated and humidified. The results showed that the still productivity was 4.921/m² day, and the decrease in airflow rate has an insignificant influence on the system productivity. Zhou et al. [6] presented a method of heat and moisture extraction from seawater under the collector of a solar chimney system for power generation and seawater desalination. They concluded that the power output from air turbine generators and water generators in the combined plant is less than that of the classic plant due to the release of vapor latent heat as the air rises up the chimney. Okati et al. [7] studied a solar desalination system with humidification–dehumidification cycle consisting of a solar humidifier and a subsurface condensation mechanism designed for producing fresh water. Brackish water is vaporized in a solar humidifier and then the humid air is passed through a set of tubes buried in the soil, then the condensation mechanism takes place and fresh water is produced. Their results showed that the rate of fresh water produced per underground pipe's length is 3.812 (kg/m h).

Okati et al. [8] presented a study of a solar water desalination system with humidification-dehumidification (HD) cycle, integrating a solar still (as a solar humidifier) and an underground condenser (dehumidifier). Their results indicated that the rate of water production could reach above 264.86 (kg/day). An increase in the inlet water temperature from 30 to 50 °C, inlet air velocity from 0.1(m/s) to 0.3 (m/s), and inlet cross – section area from 0.15 to 0.2 m² improves the productivity by 70.7%, 77.28%, and 11.39% respectively. Also decreasing the water stored in the humidifier from 6000 to 2000 kg increases the productivity from 13.05 (kg/day) to 30.74 (kg/day).

Previous studies usually either consider a uniform temperature along the glass cover of the solar distiller or considers the glass cover is only affected by the basin water temperature. The current study provided an analytical model that takes into account heat convection and mass transfer between air and glass cover. Furthermore, the temperature of the glass and air changes with both the distiller length and time.

2. Theoretical analysis

The solar distiller that considered in this steady is a longitudinal water pool covered by a transparent glass panel with an inlet for dry air and outlet for humid air as shown in Fig. 1. The solar radiation heats up the water leading to a water evaporation into the airstream. The humidity will increase gradually along the pool to reach the saturated state at a certain length depending on the evaporation rate. If the temperature of the glass cover is below the dew point of the humid air, condensation will occur on the glass. In this case, the energy balance of the solar distiller becomes:

$$Cp_f(T_{fo} - T_{fi}) + w_o h_{vo} - w_i h_{vi} = \frac{1}{\dot{m}_f} (q_{cw} + q_{ew} - q_{cg} - q_{eg}) \quad (1)$$

The subscripts i,o refer to the inlet and outlet airstream respectively and the terms q_{cw}, q_{ew} refer to convection and evaporation heat transfer between the water and airstream while the terms q_{cg}, q_{eg} refer to convection and condensation heat transfer between the airstream and glass cover. The four terms are expressed as:

$$q_{cw} = h_w A (T_w - T_f) \quad (2)$$

$$q_{ew} = \frac{h_w}{Cp_f} A h_{fg} (w_w - w_f) \quad (3)$$

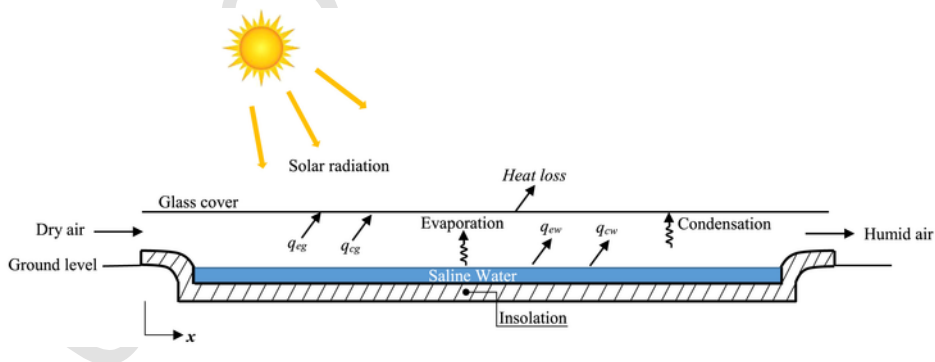


Fig. 1. The solar distiller.

$$q_{cg} = h_f A (T_f - T_g) \quad (4)$$

$$q_{eg} = \frac{h_f}{Cp_f} A h_{fg} (w_f - w_g) \quad (5)$$

The humidity ratio at water temperature of Eq. (3) is determined as [9]:

$$w_w = 0.622 \frac{P_{ws}}{P - P_{ws}} \quad (6)$$

The humidity ratio of air at water temperature w_w and air temperature T_f for an element of (dx) long through the distiller can be evaluated as follows:

$$w_w = \frac{w_i + w_o}{2} \quad (7)$$

$$T_f = \frac{T_{fi} + T_{fo}}{2} \quad (8)$$

The saturated pressure P_{ws} in Eq. (6) is calculated in term of saturated air at the water temperature as follows [10,11]:

$$P_{ws} = \exp \left(25.317 - \frac{5144}{T_w + 273} \right) \quad (9)$$

The humidity ratio at the inlet air is given as [12]:

$$w_{fi} = 0.622 \frac{\emptyset P_{fis}}{P - \emptyset P_{fis}} \quad (10)$$

where P_{fis} is the saturated pressure at the inlet air temperature, which is expressed as:

$$P_{fis} = \exp \left(25.317 - \frac{5144}{T_{fi} + 273} \right) \quad (11)$$

In addition, the humidity ratio w_g in Eq. (5) is expressed by:

$$w_g = 0.622 \frac{P_g}{P - P_g} \quad (12)$$

Where P_g is saturated pressure at the glass temperature, which is given as:

$$P_g = \exp \left(25.317 - \frac{5144}{T_g + 273} \right) \quad (13)$$

The heat transfer coefficients for water - airstream h_w and airstream-glass cover h_f are considered as follows [8,13]:

$$h_w = h_f = 2.8 + 3U_f \quad (14)$$

The latent heat of water vapor is given as [7,14]:

$$h_{fg} = 1000 (2500.8 - 2.36T_f + 0.0016T_f^2 - 0.00006T_f^3) \quad (15)$$

The enthalpy of saturated vapor at air temperature can be determined as [8,15]:

$$h_g = 1000 (2501.3 + 1.82T_f), h_v \cong h_g \quad (16)$$

The solar distiller is divided into small elements of (dx) long. The mass balance of the humid air includes the evaporation from the water layer and condensation of vapor on the glass cover:

$$w_o = w_i + \frac{\dot{m}_{ev} - \dot{m}_{co}}{\dot{m}_f} \quad (17)$$

The evaporation and condensation rates m_{ev}, m_{co} are given as [7,8,16]:

$$m_{ev} = \frac{h_w}{Cp_f} A (w_w - w_f) \quad (18)$$

$$m_{co} = \frac{h_f}{Cp_f} A (w_f - w_g) \quad (19)$$

The relative humidity of the outlet air ϕ is:

$$\phi = \frac{P_{fo}}{P_{fos}} \quad (20)$$

where P_{fo} is the vapor pressure at the outlet air temperature, which is estimated as follows:

$$P_{fo} = \frac{w_o P}{0.622 + w_o} \quad (21)$$

The saturation vapor pressure at the outlet air temperature P_{fos} is determined by:

$$P_{fos} = \exp \left(25.317 - \frac{5144}{T_{fo} + 273} \right) \quad (22)$$

Dew point of humid air can be calculated from the following relation [17]:

$$T_{dp} = \frac{243.04 \left[\ln \phi + \frac{17.625 T_f}{243.04 + T_f} \right]}{17.625 - \ln \phi - \frac{17.625 T_f}{243.04 + T_f}} \quad (23)$$

Using Eqs. (7, 17, 18) and (19), the humidity ratio of the outlet air w_o is:

$$w_o = \frac{\left[\dot{m}_f C_{pf} - \frac{A}{2} (h_w + h_f) \right] w_i + h_f A w_g + h_w A w_w}{\dot{m}_f C_{pf} + \frac{A}{2} (h_w + h_f)} \quad (24)$$

In case of no condensation $m_{co} = 0$ and the Eq. (24) becomes:

$$w_o = \frac{\left[\dot{m}_f C_{pf} - \frac{A}{2} h_w \right] w_i + h_w A w_w}{\dot{m}_f C_{pf} + \frac{A}{2} h_w} \quad (25)$$

The glass temperature shown in Eq. (4) can be estimated using heat and mass balance for the glass cover as follows:

$$I (1 - \tau_g) \alpha_g + h_f (T_f - T_g) + \frac{h_f}{Cp_f} h_{fg} (w_f - w_g) = h_a (T_g - T_a) \quad (26)$$

The glass temperature becomes:

$$T_g = \frac{I (1 - \tau_g) \alpha_g + h_f T_f + \frac{h_f}{Cp_f} h_{fg} (w_f - w_g) + h_a T_a}{h_f + h_a} \quad (27)$$

The outside heat transfer coefficient h_a is given as [18,19]:

$$h_a = 5.7 + 3.8 U_a \quad (28)$$

In case of no condensation ($T_g > T_{dp}$); the term $\frac{h_f}{Cp_f} h_{fg} (w_f - w_g)$ disappears in Eq. (27) and the glass temperature becomes:

$$T_g = \frac{I (1 - \tau_g) \alpha_g + h_f T_f + h_a T_a}{h_f + h_a} \quad (29)$$

The solar radiation incident on the distiller consists of two components: direct and diffused, the direct solar can be given by [20]:

$$I_{dr} = I_{sc} \tau^{m_a} \sin \beta \quad (30)$$

where I_{sc} is the solar constant (1367 W/m²)

In addition, the diffused solar radiation is given as:

$$I_{df} = 0.3I_{sc} (1 - \tau^{m_a}) \sin \beta \quad (31)$$

The total solar radiation incident on the distiller is the summation of the direct and diffused components:

$$I = I_{dr} + I_{df} \quad (32)$$

The altitude angle (β) can be evaluated from the following relation [21]:

$$\sin \beta = \cos \ell \cos \lambda \cos \delta + \sin \ell \sin \delta \quad (33)$$

where τ is the atmospheric transmittance, it is between 0.65 and 0.75 [20]. In this work, τ was taken as 0.7.

The air mass (m_a) is determined as [22]:

$$m_a = \frac{1}{\sin \beta} \quad (34)$$

The hourly ambient temperature along the day is determined using the following formulas [23]:

For day

$$T_a = T_{a,\min} + (T_{a,\max} - T_{a,\min}) \sin \left(\frac{\pi t}{y + 3.6} \right) \quad (35)$$

For night

$$T_a = T_{a,\min} + (T_{sunset} - T_{a,\min}) \exp \left(-2.2 \frac{t - y}{24 - y} \right) \quad (36)$$

where y is the day length

The outlet air temperature T_{fo} can be deduced from Eq. (1) using Eqs. (2, 4), and (8) as follows:

$$T_{fo} = \frac{\left[\dot{m}_f C_{pf} - \frac{A}{2} (h_w + h_f) \right] T_{fi} + \dot{m}_f (w_i h_{vi} - w_o h_{vo}) + h_f A T_g + h_w A T_w + q_{ew} - q_{eg}}{\dot{m}_f C_{pf} + \frac{A}{2} (h_w + h_f)} \quad (37)$$

In case of no condensation on the glass cover where the glass temperature is higher than the dew point temperature of the air ($T_g > T_{dp}$), the term q_{eg} disappears from the Eq. (37). Solving the Eqs. (24, 25), and (37) to determine, the air temperature and humidity ratio in each element (dx) for a given water temperature T_w along the distiller. The water temperature T_w can be estimated as a function of time using the following time - dependent energy balance of the water layer:

$$M_w C_w \frac{dT_w}{dt} = I \alpha_w \tau_g A - h_w A (T_w - \bar{T}_f) - \frac{h_w}{C_{pf}} A h_{fg} (w_w - \bar{w}_f) \quad (38)$$

The average air temperature and humidity ratio along the distiller are determined by numerical integration technique as follows:

$$\bar{T}_f = \frac{1}{L} \int_0^L T_f dx \quad (39)$$

$$\bar{w}_f = \frac{1}{L} \int_0^L w_f dx \quad (40)$$

3. Results and discussion

The performance of a solar distiller is theoretically analyzed according to the climate conditions in one of the hottest zones in the world (Basra, Iraq). The inlet parameters used in the calculations are tabulated in Table 1.

The hourly solar radiation was theoretically estimated and the ambient temperature has been taken from the world weather online records for Basra city throughout the year. Eq. (38) was solved numerically using Euler method with a time interval of (300 s) to evaluate the water temperature as a function of the local time. Furthermore, the Eqs. (24, 25), and (37) are resolved by dividing the solar distiller into small elements of (dx) long to evaluate air temperature and humidity ratio at any location and any time along the distiller. Fig. 2 explained an increase in the evaporation rate with increasing the air velocity; this is due to the increase of heat and mass transfer coefficient as the air velocity increases. The gradient of the evaporation rate gradually decreasing along the distiller because of increasing the relative humidity, which in turn decreases the evaporation potential. Fig. 3 shows the fresh water production of the system considered. The productivity starts (condensation) when the glass cover temperature just equal to or less than the dew point of the humid air. It is noted that the productivity starts earlier at the lower air velocity (about 7.4 m away from

Table 1
Inlet Parameters.

Parameter	value
Air velocity	0.15 m/s
Width of the distiller	1 m
height of the distiller	0.5 m
Wind velocity	5 m/s
Inlet relative humidity	10%
Water absorptivity	0.9
glass absorptivity	0.1
Air density	1.15 kg/m ³
Air specific heat	1005 J/kg K
Water density	1000 kg/m ³
Water specific heat	4200 J/kg K
Water layer height	0.1 m
Latitude	30.5°
Longitude	47.8°

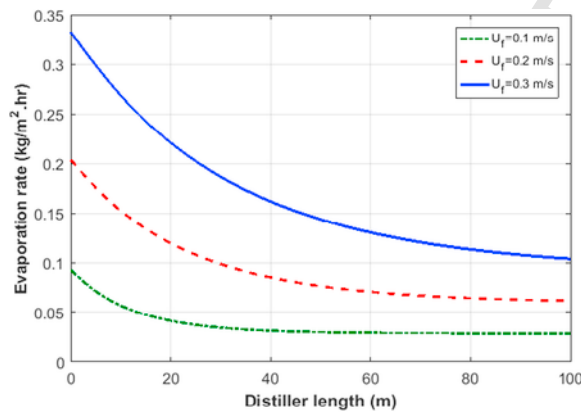


Fig. 2. Variation of evaporation rate for different values of air velocity.

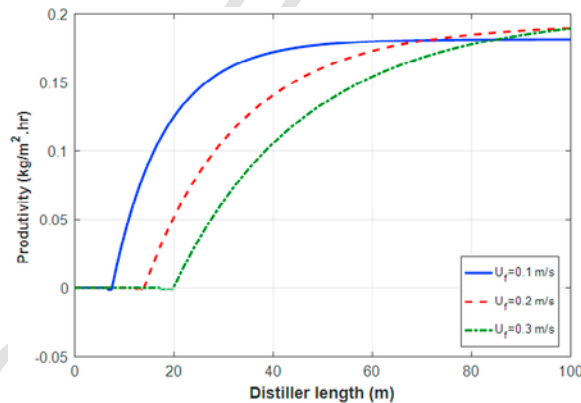


Fig. 3. Effect of air velocity on the productivity along the distiller.

the distiller entrance at $U_f = 0.1$ m/s and 20 m when $U_f = 0.3$ m/s since the glass temperature is less at low velocity due to less amount of heat transfers to the glass cover.

In spite of the increase in the evaporation rate with the increase of the air velocity inside the distiller, the productivity decreases as it clear in Fig. 4. This can be explained as: the increase in air velocity leads to an increase in the heat transfer to the glass cover, which decreases the condensation potential on the cover. Fig. 5 indicated the results of the fresh water production throughout the year. It is clear that the productivity inversely proportional to the air velocity inside the distiller and it has maximum value 2.2 kg/m² day on March and fall to 0.66 kg/m² day on July at air velocity 0.1 m/s and approaches zero for air velocity 0.3 m/s in spite of the higher solar radiation, water temperature, and evaporation rate. This is because the glass temperature along the daylight period is higher than the dew, point of the humid air in July.

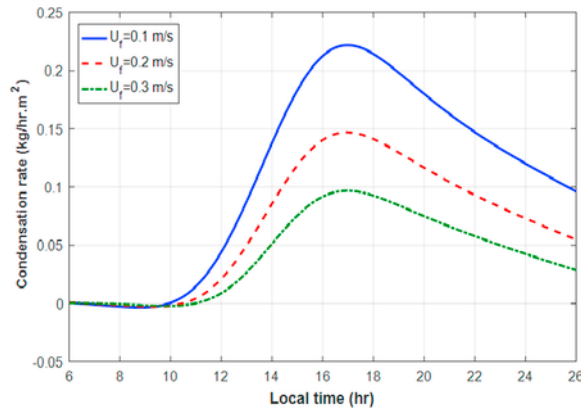


Fig. 4. Variation of condensation rate within a day for different values of air velocity.

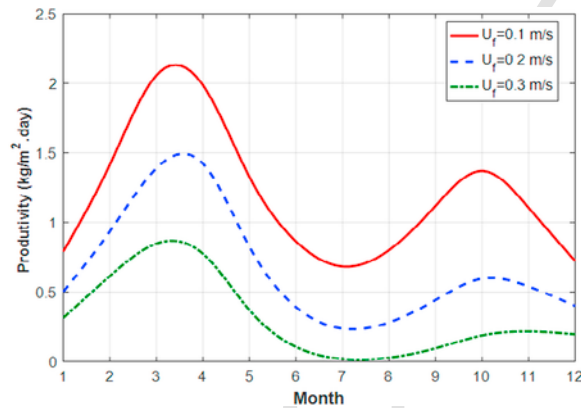


Fig. 5. Productivity profile within a year for different values of air velocity.

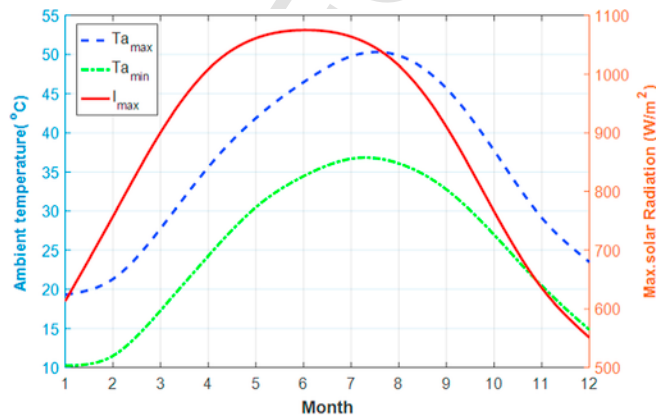


Fig. 6. Maximum solar radiation incident on the distiller with maximum and minimum ambient temperatures within a year.

Fig. 6 illustrates the monthly maximum solar radiation incident on the distiller calculated by using Eq. (32) for the location (latitude 30.5° , Longitude 47.8°). The highest value of the solar radiation determined in June due to the highest altitude angle at mid-day ($\beta \cong 83^\circ$). Furthermore, the figure explains the maximum and minimum ambient temperatures according to the considered Basra climate conditions in the calculations. Fig. 7 shows the evaporation rate of the current analysis and the works by Sartori [4] and Okati [8] for same inlet air velocity ($U_i = 0.1$ m/s) and similar water temperature variation with time which is reached a maximum value of 66°C . The percentage differences between the current work and Refs. [4,8] are 9.28% and 8.94% respectively. The comparison provides validity evidence of the present work.

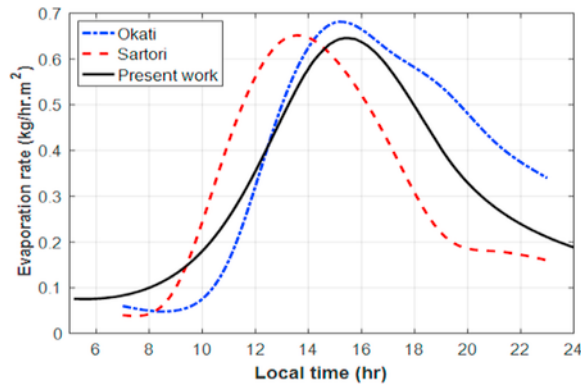


Fig. 7. Comparison of a daily evaporation rate of the present work and the works by Okati [8] and Sartori [4].

4. Conclusions

1. The productivity of freshwater has a maximum value during March and reach a minimum value in July.
2. The productivity decreases with increasing air velocity inside the distiller while the evaporation rate increases.
3. The air velocity inside the distiller has a significant effect on the productivity.
4. The low productivity at high air velocity is due to the latent and sensible heats transfer to the glass cover.

References

- [1] H.M. Ali, Experimental study on the air motion effect inside the solar still on still performance, *Energy Convers. Manag.* 32 (1) (1991) 67–70.
- [2] H.M. Ali, Mathematical model of the solar still performance using forced convection with condensation process outside the still, *Renew. Energy* 1 (5/6) (1991) 709–712.
- [3] H.M. Ali, Effect of forced convection inside the solar still on heat and mass transfer coefficients, *Energy Convers. Manag.* 34 (1) (1993) 73–79.
- [4] Emani Sartori, Solar still versus solar evaporator: a comparative study between their thermal behaviors, *Sol. Energy* 56 (2) (1996) 199–206.
- [5] Abdulhaiy M. Radhwan, Transient analysis of a stepped solar still for heating and humidifying greenhouses, *Desalination* 161 (2004) 89–97.
- [6] Xiping Zhou, Bo Xiao, Wanchao Liu, Xianjun Guo, Jiakuan Yang, Jian Fan, Comparison of classical solar chimney power system and combined solar chimney system for power generation and seawater desalination, *Desalination* 250 (2010) 249–256.
- [7] V. Okati, A. Behzadmehr, S. Farsad, Analysis of a solar desalinator (humidification–dehumidification cycle) including a compound system consisting of a solar humidifier and subsurface condenser using DoE, *Desalination* 397 (2016) 9–21.
- [8] V. Okati, S. Farsad, A. Behzadmehr, Numerical analysis of an integrated desalination unit using humidification-dehumidification and subsurface condensation processes, *Desalination* 433 (2018) 172–185.
- [9] E.H. Amer, H. Kotb, G.H. Mostafa, A.R. El-Ghalban, Theoretical and experimental investigation of humidification–dehumidification desalination unit, *Desalination* 249 (2009) 949–959.
- [10] S.W. Sharshir, Guilong Peng, Nuo Yang, Mohamed A. Eltwil, Mohamed Kamal Ahmed Ali, A.E. Kabeel, A hybrid desalination system using humidification-dehumidification and solar stills integrated with evacuated solar water heater, *Energy Convers. Manag.* 124 (2016) 287–296.
- [11] C. Elango, N. Gunasekaran, K. Sampathkumar, Thermal models of solar still—a comprehensive review, *Renew. Sustain. Energy Rev.* 47 (2015) 856–911.
- [12] Mofreh H. Hamed, A.E. Kabeel, Z.M. Omara, S.W. Sharshir, Mathematical and experimental investigation of a solar humidification–dehumidification desalination unit, *Desalination* 358 (2015) 9–17.
- [13] Emani Sartori, Convection coefficient equations for forced air flow over flat surfaces, *Sol. Energy* 80 (2006) 1063–1071.
- [14] R.R. Rogers, M.K. Yau, *A Short Course in Cloud Physics*, Pergamon Press, 1989.
- [15] Yunus A. Cengel, Michael A. Boles, *Thermodynamics: An Engineering Approach*, 3rd ed., McGraw-Hill, 2001.
- [16] B. Molineaux, B. Lachal, O. Guisan, Thermal analysis of five outdoor pools heated by unglazed solar collectors, *Sol. Energy* 53 (1) (1994) 21–26.
- [17] Mark G. Lawrence, The Relationship between relative humidity and the dew point temperature in moist air: a simple conversion and applications, *Bull. Am. Meteorol. Soc.* 86 (2) (2005) 225–233.
- [18] Hassan E.S. Fath, Samy Elsherbiny, Ahmad Ghazy, A naturally circulated humidifying/dehumidifying solar still with a built-in passive condenser, *Desalination* 169 (2004) 129–149.
- [19] Salman H. Hammadi, Tempering of water storage tank temperature in hot climates regions using earth water heat exchanger, *Therm. Sci. Eng. Prog.* 6 (2018) 157–163.
- [20] Y. El Mghouchi, E. Chham, M.S. Krikiz, T. Ajzoul, A. El Bouardi, On the prediction of the daily global solar radiation intensity on south-facing plane surfaces inclined at varying angles, *Energy Convers. Manag.* 120 (2016) 397–411.
- [21] Y. El Mghouchi, A. El Bouardi, Z. Choulli, T. Ajzoul, Models for obtaining the daily direct, diffuse and global solar radiations, *Renew. Sustain. Energy Rev.* 56 (2016) 87–99.
- [22] N. Nijegorodov, P.V.C. Luhanga, Air mass analytical and empirical treatment an improved formula for air mass, *Renew. Energy* 7 (1) (1996) 57–65.
- [23] D.C. Reicosky, L.J. Winkelman, J.M. Baker, D.G. Baker, Accuracy of hourly air temperatures calculated from daily minima and maxima, *Agric. For. Meteorol.* 46 (1989) 193–209.